Astron. Astrophys. 317, L13–L16 (1997)

ASTRONOMY AND ASTROPHYSICS

LETTER

Letter to the Editor

RX J0911.4+0551: A new multiple QSO selected from the ROSAT All-Sky Survey⋆

Norbert Bade[1], **Joachim Siebert**[2], **Sebastian Lopez**[1], **Wolfgang Voges**[2], **and Dieter Reimers**[1]

[1] Hamburger Sternwarte, Gojenbergsweg 112, D-21029 Hamburg, Germany
[2] MPI für Extraterrestrische Physik, D-85740 Garching, Germany

Received 19 September 1996 / Accepted 14 November 1996

Abstract. We report from follow-up observations of high redshift AGN candidates from the ROSAT All-Sky Survey (RASS) that RX J0911.4+0551 is a gravitationally lensed QSO with z = 2.800. With an X-ray luminosity of $L_X = 4 \cdot 10^{46}$ ergs s^{-1} it belongs to the X-ray brightest radio quiet QSOs. However, we must point out that the existing observations do not exclude the possibility that other objects inside the error circle are responsible for the X-ray flux, in particular a lensing cluster. Careful image analysis discerned three optical images. The separation between the two brighter components of 0.″80 is below the seeing value during the observations. The fainter component has a distance of 3.″1. The spectra of the brighter joint A, B component and the C component show no measurable differences in continuum and absorption lines. Three strong CIV absorption line systems with $W_\lambda(1549) > 1$ Å are visible in the spectra. All three have $z > 2.3$ which makes it improbable that they are caused by the lensing systems. The only spectral difference are larger equivalent widths of the broad emission lines in the brighter QSO components.

Key words: Quasars: general - Quasars: individual: RX J0911.4+0551 - Gravitational lensing

1. Introduction

Gravitationally lensed QSOs allow in principle an independent measurement of the Hubble constant (Refsdal, 1964) and the investigation of dark matter in the lensing objects (galaxies and / or clusters of galaxies). Bright multiple QSOs have also become important for studying the spatial extent of intervening absorbing clouds. Therefore, large efforts have been undertaken to select such objects, especially since the discovery of the double QSO Q 0957+561 (Walsh et al., 1979) for which convincing arguments can be given that its double image is caused by gravitational lensing.

The gravitationally lensed QSOs known so far were found by follow-up observations of optically or radio selected objects. RX J0911.4+0551 was found by a large identification program of RASS sources on Schmidt plates from the Calar Alto Schmidt telescope (Bade et al., 1995, Hagen et al., 1995). The objective prism plates, relevant for the recognition of the AGN nature of the optical counterparts, have a limiting magnitude of B = 18.5 and at low ecliptic latitudes the RASS comprises X-ray sources down to $f_X(0.1 - 2.4\mathrm{keV}) = 2 \cdot 10^{-13}$ ergs cm^{-2} s^{-1} (Voges, 1992). Thus, RX J0911.4+0551 was selected by the combination of two large area surveys in the optical and X-ray wavelength band. The magnification bias causes lensed QSOs to be more abundant among the brightest objects in a flux limited sample (Surdej et al., 1993). This bias is even enhanced if the selection is done in two widely separated wavelength bands (Borgeest et al., 1991).

From lens theory an odd number of images is expected. Nevertheless, nearly all known examples of multiple QSOs have an even number of images (2 or 4). This can be explained with demagnification of one image in the core of the lens (Narayan et al., 1984). Only Q 2016+112 seems to have 3 images, but in radio observations by Garrett et al. (1996) one of the images splits up into three components. Wallington and Narayan (1993) have shown that the magnification bias is considerably stronger in the case of quadruples. The portion of quadruples to doubles should decrease in deeper lens surveys.

2. Observations

2.1. Discovery

RX J0911.4+0551 is a weak RASS source with 0.02 cts s^{-1}. At a distance of 21″ (see Fig. 1) the plausible optical counterpart

Send offprint requests to: Norbert Bade

⋆ Based on observations made at the European Southern Observatory, La Silla, Chile

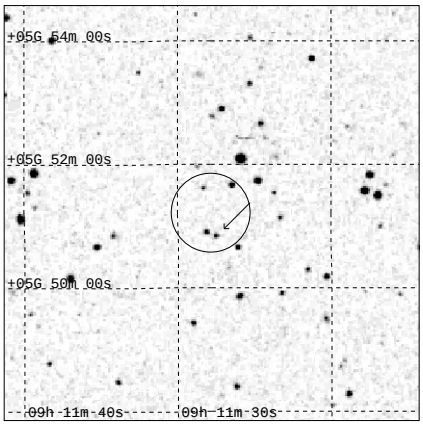

Fig. 1. Finding chart for RX J0911.4+0551 taken from digitized POSS. The circle shows the error radius of the X-ray position. The QSO is marked with an arrow (optical position α = 09h 11m 27.5s $\delta = 05^\circ\ 50'\ 52''$, equinox 2000.0). Only marginal hints of its multiple character are visible in this image

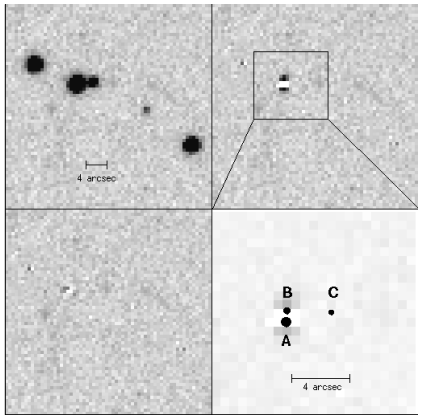

Fig. 2. The upper left panel is a cut of the EFOSC I Johnson R CCD frame with an exposure time of 60 s and limiting magnitude of R = 22 around RX J0911.4+0551. In the upper right panel the QSO was assumed as double and the fitted objects were subtracted. Strong deviations from random noise remain around the brighter QSO component, which disappear if 3 images are assumed for the QSO (lower left panel). The enlargement in the lower right panel shows the positions of the fitted QSO images

Table 1. Geometry and brightnesses of the components derived with DAOPHOT. $\triangle\alpha$ and $\triangle\delta$ give the coordinates with respect to component A, $\triangle \mathrm{mag_R}$ the magnitude difference, respectively. Results of both observations are given, the April 1996 value on the left side and the December 1995 on the right. The deviations are within the statistical errors, only the differing values of $\triangle \mathrm{mag_R}$ between A and C indicate real variability. The December 1995 observations lead to R = 18.05 ± 0.05 for the A component and an integrated R = 17.34 ± 0.05

Comp.	$\triangle\alpha$		$\triangle\delta$		$\triangle \mathrm{mag_R}$	
	EFOSC	DFOSC	EFOSC	DFOSC	EFOSC	DFOSC
A	0.00	0.00	0.00	0.00	0.00	0.00
B	-0.05	-0.12	0.77	0.77	0.64	0.56
C	-3.09	-3.18	0.66	0.59	1.42	1.21

of RX J0911.4+0551 was identified as a QSO candidate with z = 2.8 on Calar Alto objective prism plates. We note that reliable redshift estimates for AGN candidates on IIIa-J objective prism plates are only possible for AGN with strong emission lines, especially the Ly-α line for QSOs with $z > 1.8$. No other plausible optical counterpart was found in the error circle of RX J0911.4+0551. Existing radio catalogues have no entry at this position, including the NRAO/VLA Sky Survey (NVSS, Condon et al., 1993). The low statistics allow no spectral analysis. Assuming the QSO as the X-ray source and a power law spectrum with photon index Γ = 2.2 (as found by Reimers et al. (1995) for high redshift radio quiet QSOs) and only Galactic aborption leads to $f_X = 2 \cdot 10^{-13}$ ergs cm^{-2} s^{-1} in the ROSAT band. In December 1995 a spectrum with 20 min integration time taken with the 1.54m Danish telescope equipped with DFOSC confirmed the classification as a QSO with z = 2.80. This leads to a X-ray luminosity of $L_X = 4 \cdot 10^{46}$ ergs s^{-1} in the ROSAT band (H_0 = 50 km s^{-1} Mpc^{-1}, q_0 = 0). The direct image taken for acquisition purposes revealed a faint companion not visible on the objective prism and direct Schmidt plates. The spectrum of this object had only very low signal to noise but did show stronger signal at the broad emission line position of the QSO. Additional spectra, taken with DFOSC (55 min exposure time) and in April 1996 with EFOSC I (30 min exposure) confirmed that the companion was a QSO with the same redshift. The EFOSC I spectra have an effective resolution of 21 Å (FWHM) and the DFOSC spectra of 11 Å.

2.2. Imaging and photometry

The DFOSC acquisition exposures were also used for photometry. The CCD frames were calibrated by taking E3 regions Johnson B and R CCD frames at least twice per night. In December 1995 the CCD of DFOSC had a very steep quantum efficiency curve between 4000 and 5000 Å (nearly insensitive for $\lambda < 4000$Å). Therefore we give here only B = 18.34 for the joint A, B component derived from the April 1996 spectrum.

The program DAOPHOT in the MIDAS environment was used to calculate a mean PSF on the CCD frame, necessary to decompose the images. The faint companion of RX J0911.4+0551 and the neighbouring stars were described adequately by the calculated PSF, the subtraction of the fitted PSF produced only random noise. For the brighter component this procedure leads to significant remaining signal north and south of the fitted PSF position (20 σ largest deviation on EFOSC I frame). The largest deviation from random noise was found near the peak of the QSO image, it was strongly overfitted so that the subtraction of the PSF provided a value considerably (73 σ) below the sky background (see also Fig. 2).

We take this result as evidence that the brighter QSO component splits up into two components and repeated the PSF fitting with the DAOPHOT program under this assumption, from which a distance of 0.″8 was obtained for the brighter components. This has to be compared with the seeing of 1.″4 for both the DFOSC and EFOSC I observations. The subtraction of the fitted PSF images provides satisfying results for the three components (Fig. 2). The positional and photometric results agree

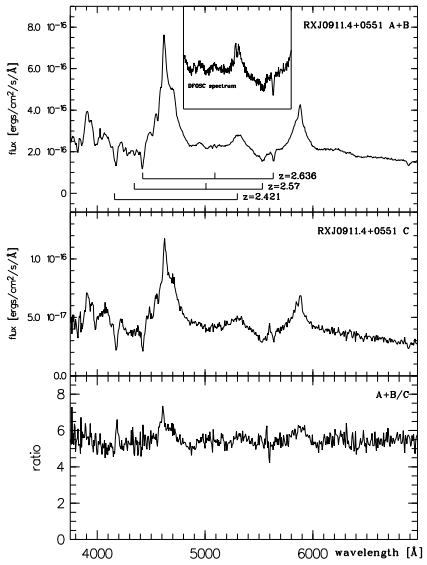

Fig. 3. The upper and middle panel show the EFOSC I spectra of the joint component A+B and C. The lower panel shows the flux ratio of A+B to C. Three strong absorption line systems are marked in the upper panel. The inset in the upper panel shows the DFOSC spectrum of the A+B component with an offset of $5 \cdot 10^{-16}$ ergs cm^{-2} s^{-1}, there the absorption lines are better resolved

formally for the EFOSC I and DFOSC Johnson R CCD frames. In Tab. 1 the photometric results and distances of the QSO components from each other are summarised for both observations.

The stable fit result obtained on two independent CCD frames together with the small brightness difference between the brighter QSO components makes us believe in the existence of at least 3 components. If the same result was obtained in another independent colour, a galaxy or a serendipitous star companion could be more thoroughly excluded. Our DFOSC Johnson B frames had not enough signal to do this job, nevertheless the B frames are consistent with our assumption. Additionally, the spectral results strongly support 3 components.

2.3. Spectral properties

Spectra of the unresolved A+B and the C component were taken simultaneously with the slit in E-W orientation. In both cases a slit width of 5″ was used to avoid slit losses. The seeing conditions were only moderate and therefore the joint A, B and the weaker component C overlap slightly. In order to leave as little mutual interference as possible we used a procedure to extract the two spectra by fitting simultaneously two Gaussian profiles to the data. The procedure is described in more detail in Smette et al. (1995). Wavelength calibration was performed with exposures of He-Ar standard lamps. Due to weak signal of the standard lamp below 4200Å the wavelength scale of the DFSOC spectrum is uncertain below this value. An intensity calibration was obtained by observing spectrophotometric standard stars, GD 108 for EFOSC I and Hiltner 600 for DFOSC. The EFOSC I spectra are shown in Fig. 3.

The redshift was determined by fitting a Gaussian to the Ly-α and CIV emission line. For the joint A, B component we measure an average value of z = 2.799 for the two observations and z = 2.801 for the C component. This redshift difference is small, 158 km s^{-1} in the rest frame of the QSO, and if the width of the emission lines is considered (FWHM is more than ten times larger), both redshift values are consistent with each other. Besides Ly-α and CIV strong emission lines from OVI/Ly-β, NV 1240, CII 1334, SiIV 1398 and CIII] 1909 are discernible (the latter only in the DFOSC spectra).

If the joint A, B EFOSC I spectrum is divided by the spectrum of component C, a nearly constant value (5.47) is obtained for the continuum over the whole spectral range (Fig. 3). Variations on large wavelength scales cannot be detected, which argues for the same continuum in the different components. The flux ratio of the Ly-α, NV and the CIV emission lines between the joint A+B component and the weaker component C of 5.81 is considerably higher than in the continuum, which is confirmed by the noisier but higher resolution DFOSC spectra. In the line core of Ly-α the flux ratio rises even to 7.35. This result is opposite to what has been found in HE 1104-1805 (Wisotzki et al., 1993). In this double QSO the weaker component shows stronger emission lines and the brighter component has a steeper spectral slope. The authors take their findings as evidence for microlensing in the brighter component.

Three absorption line systems can be recognized in the optical spectra, all with no measurable differences between the A+B and the C component. The absorption system at z = 2.636 has strong CIV 1549 absorption ($W_{\lambda_{\rm rest}}(1549)$ = 1.7Å), SiIV 1398 and Ly-α absorption. The CIV 1549 absorption of the z = 2.421 system coincides serendipitously with the SiIV 1398 emission line and is more readily distinguishable in the DFOSC spectrum, the identification is supported by the strong Ly-α absorption at 4160 Å. Of special interest is the absorption at 5546 Å, which spans 60 Å (FWHM 41 Å), corresponding to 3200 km s^{-1}. If this absorption was identified with CIV 1549, it would mean z = 2.57 with $W_{\lambda_{\rm rest}}(1549)$ = 2.7Å; because of the ill defined continuum in this region this value is a lower limit. The redshift is supported by a similarly shaped SiIV 1398 absorption, while the corresponding Ly-α absorption is rather weak. Although the absorption system has not the strength of a typical BAL, it fulfills the other characteristics of BALs (Weymann et al., 1991). The other two absorption systems have also large CIV 1549 equivalent widths, comparable to the highest values found by Sargent et al. (1988).

The common view is that BALs are caused by high velocity outflow from the QSO itself (Weymann et al., 1991), on the other hand high ionisation metal absorption systems belong to galactic halos. One of the absorption systems might be associated with the lensing system (galaxy and/or cluster of galaxies), although this is rather unlikely. The absorption redshifts are close to the emission redshift of the QSO. The mass of the lensing system is approximately inversely proportional to the angular diameter distance between QSO and deflector. In the case of RX J09114+0551 extremely high masses (of the order 10^{14} M$_\odot$) would be needed for the lensing system close to the QSO to explain the configuration of the QSO images.

3. Discussion and conclusions

The two separate optical spectra show striking similarity. Between 3800 Å and 6900Å the continua show no distinct deviations from each other. We therefore suggest that RX J0911.4+0551 is split into multiple images by gravitational lensing. Strong support for this explanation comes from the double nature of the brighter component. Separate optical spectra of these two tight QSO images do not exist, but the similarity of the joint A, B component spectrum to the weaker C spectrum makes it difficult to find another interpretation for the close pair. This is enhanced by the additional agreement between the absorption line systems in the two optical spectra. The close companion of the brighter QSO cannot be a galaxy or a serendipitous star since in this case the absorption lines would be weakened in the combined spectrum. It should be noted that strong absorption line systems need not be equal in the different QSO images, as found here, for the gravitationally lensing interpretation; HE 1104-1805 (Wisotzki et al., 1993) is a counterexample.

The only measurable difference between the two optical spectra was found in the equivalent widths of the broad emission lines. The joint A, B component has stronger emission lines, in reverse to the situation found in HE 1104-1805. The latter case was explained with microlensing in the bright component. RX J0911.4+0551 is a more complex system; a possible explanation could be a microlensing event in component C which caused a stronger magnification of the continuum source because of its smaller angular extent. This rather speculative explanation finds support in the variability of companion C (Tab. 1). However, this result needs to be confirmed by future photometric and spectroscopic observations.

A further open question is the exact geometry of the QSO images. The hitherto existing observations have revealed 3 images. Nearly all other known gravitationally lensed QSO show two or four images. Although the PSF fitting of the system gives acceptable results with three images, the deviations from random noise are slightly larger compared to the neighbouring stars if the fitted PSFs are subtracted. More detailed observations will show whether these deviations are real and can be attributed to a fourth image or the lensing system.

Three strong CIV absorption line systems can be discerned, all relatively close to the emission line redshift. This makes it unprobable that they originate from the lensing system, because this would lead to unreasonably high lensing masses. The absorption line system at z = 2.57 has broad absorption lines, but is rather weak for a BAL. Higher resolution spectra will clarify the classification. The up to now tentative BAL interpretation could be important in the X-rays, since previous observations have shown that BAL QSOs are strongly absorbed in soft X-rays (Mathur et al., 1996, Green and Mathur, 1996). However, RX J0911.4+0551 was selected by the RASS, a soft X-ray survey sensitive between 0.1 and 2.4 keV.

High redshift QSOs are rare in the RASS (Bade et al., 1995), in particular radio quiet QSOs. In the soft X-ray region region most of the $z > 2$ QSOs are radio loud (Yuan et al., 1996). A preliminary correlation of the RASS with the Véron AGN catalogue (Véron-Cetty and Véron, 1993) revealed only eight radio quiet QSOs with $z > 2$ and more than $0.03\,\mathrm{cts\,s^{-1}}$, including another gravitationally lensed QSO (HE 1104−1805). This also means that most high redshift radio quiet QSO have not been detected in the RASS and lets us think about alternative sources for the X-ray flux in the error circle. If such a source could be found the double magnification bias (Borgeest et al., 1991) is not applicable for RX J0911.4+0551. In the case of a multiple QSO a lensing cluster with $z \gtrsim 0.5$ could be responsible for the X-rays. A single normal galaxy acting as the lens can be excluded as an X-ray source since a galaxy with $B > 22$ is too weak in the X-ray band. A possible cluster in front of RX J09114+0551 should be revealed by its extended X-ray emission and its different spectral behaviour. For both characteristics the collected 10 source photons are too few, only more sensitive X-ray observations can exclude a cluster as the X-ray source. However, pointed ROSAT observations have already proven that radio quiet QSOs of comparable X-ray luminosity exist (HS 1700+6416, Reimers et al., 1995).

The RASS will detect only the brightest high redshift radio quiet QSOs. The selection of additional such objects could provide further gravitationally lensed QSOs. Objective prism plates can serve as a cheap tool to select these QSOs since their characteristic strong Ly-α emission lines enable their discovery up to $z \approx 3.2$ with IIIa-J emulsion, provided the QSOs are optically bright enough ($B \lesssim 18$).

Acknowledgements. The ROSAT mission was supported by the Ministerium für Forschung und Technologie (BMFT) and by the Max-Planck-Gesellschaft. We thank S. Refsdal and L. Wisotzki for valuable discussions. We are also indebted to S. Köhler who took the EFOSC spectra. This work has been funded by the Deutsche Forschungsgemeinschaft under Re 353/22-1 to 4 and by BMBF under DARA/Reimers 50 0R 96016.

References

Bade N., Fink H.H., Engels D., et al., 1995, A&AS 110, 469
Borgeest U., v. Linde J., Refsdal S., 1991, A&A 251, L35
Condon J.J., Cotton W.D., Greisen E.W., et al., 1993, BAAS 183, 6402
Garrett M.A., Porcas R.W., Nair S., Patnaik A.R., 1996, MNRAS 279, L7
Green P.J., Mathur S., 1996, ApJ 462, 637
Hagen H.-J., Groote D., Engels D., Reimers D., 1995, A&AS 111, 195
Mathur S., Elvis M., Singh K.P., 1996, ApJ 455, L9
Narayan R., Blandford R.D., Nityanada R., 1984, Nature 310, 112
Refsdal S., 1964, MNRAS 128, 307
Reimers D., Bade N., Schartel N., et al., 1995, A&A 296, L49
Sargent W.L. W., Boksenberg A., Steidel C. C., 1988, ApJS 68, 539
Smette A., Robertson J.G., Shaver P.A., et al., 1995, A&AS 113, 199
Surdej J., Claeskens J.F., Crampton D., et al., 1993, AJ 105, 2064
Véron-Cetty M.-P., Véron P. 1993, ESO Sci. Rep. No 13
Voges W. 1992, in Proceedings on European International Space Year Meeting ESA ISY-3, 9
Wallington S., Narayan R., 1993, ApJ 403, 517
Walsh D., Carswell R., Weymann R., 1979, Nature, 279, 381
Weymann R.J., Morris S.L., Foltz C.B., Hewett P.C., 1991, ApJ 373, 23
Wisotzki L., Köhler T., Kayser R., Reimers D., A&A 278, L15
Yuan W., Brinkmann W., Siebert J., Voges W., A&A submitted